Dissolution Study on Aspirin and α-Glycine Crystals

Hong Wen, Tonglei Li, Kenneth R. Morris,* and Kinam Park

Department of Industrial and Physical Pharmacy, Purdue University, West Lafayette, Indiana 47907-1336

Received: August 4, 2003; In Final Form: April 28, 2004

The broad objective of this research is to better understand the dissolution processes of drug crystals in the molecular level, especially the interactions between solvent molecules and drug molecules at the interface. For aspirin and α-glycine crystals, the (100) face of aspirin and the (010) face of α-glycine were used for partial dissolution studies. The etching patterns for both aspirin and α-glycine reflect the directionality and strength of the attachment energies projected onto the faces of interest very well, and the predicted etching patterns match observed etching patterns well especially for solvents with weak and moderate solubilizing ability. These results further support our conclusions from earlier publications that surface diffusion, guided by the directional attachment energies, is the primary architect of etching pattern morphology. The solubilizing ability of solvents can significantly affect the surface diffusion time of the involved molecules. In the directions of the dominant attachment energies, the etching patterns in solvents with high solubilizing ability (e.g., pyridine, acetone) become less pronounced than the etching patterns in solvents with low ability (e.g., dichloroethane). Surface adsorption of the solvent also plays an important role in etching pattern formation. In α-glycine crystals, acetone may form hydrogen bonds with glycine and introduces certain anisotropy in the relatively deeper etched pits, i.e., oval etching patterns whose basic directionality is, however, still controlled by attachment energy network. Overall, the formation of etching patterns is mainly determined by attachment energies that are important in guiding surface diffusion, and is also affected by solvents with different solubilizing ability and surface adsorption potential.

Introduction

In our continuing efforts to elucidate the dissolution process, aspirin and glycine were chosen as model compounds based on structural considerations. Aspirin has only one known crystal form even though there are other potential polymorphs predicted by computational methods.[1] Glycine has three crystal forms: α-, β-, and γ-glycine with respective space groups $P2_{1/n}$, $P2_1$, and $P3_1$ or $P3_2$.[2−4] Among the three forms, β-glycine is the least stable at room temperature while the other two forms are relatively stable at room temperature.[5] The α-glycine used here can be grown from saturated aqueous solution by slowly evaporating solvent.[2] Aspirin has been widely studied for its dissolution properties, especially the relationship between dissolution rate and crystal habit. It has been reported that the rate of material flux from the (100) face is about 6 times greater than that from the (001) face.[6−8] Consistent with this observation is that dynamic chemical force microscopy studies show that the (100) face has greater interaction with a hydrophobic tip than the (001) face, and the (001) face has greater interaction with a hydrophilic tip than the (100) face.[9]

Both aspirin and α-glycine crystals consist of two-dimensional layers stacked along the third dimension interacting through van der Waals forces; hydrogen bonding is the dominant interaction within the layers. By cleaving crystals of each compound, a smooth surface can be produced and used to study the effects of crystal structure and solvent on the shape of etching patterns. The hydrogen bonds in aspirin crystals do not form hydrogen bond chains, but exist between the two molecules comprising an aspirin dimer.[10] In crystal structures such as that of acetaminophen (the subject of our earlier work), the hydrogen bonds form networks. The network structure (e.g., hydrogen bond chains in acetaminophen), typically plays a more important role in the formation of etching patterns than in systems such as aspirin.[11] The crystal structure of α-glycine also contains a hydrogen bond network, with more hydrogen bond chains, i.e., a more extensive network, than the acetaminophen monoclinic crystal. By choosing these two crystal structures with different hydrogen bonding properties, the effect of solvent adsorption onto the crystal surface through hydrogen bonding between the solvent and drug molecules on the crystal surface was studied.

Li et al. conducted etching studies on the (010) face of acetaminophen crystals using various solvents,[11] and surface textures and etching patterns were observed with an atomic force microscope (AFM). Based on the crystal structure, a model was proposed for the simulation of the dissolution process. Two essential events were considered during simulation: detachment and surface diffusion of an acetaminophen molecule. Simulation results indicated that surface diffusion plays a key role in forming the etching patterns. It was found that the diffusion of surface molecules was guided or confined by the underlying crystal structures, especially the supramolecular interaction network. The effects of crystal structure on the formation of the etching patterns are mainly through the guiding influence of the attachment energy "network" on surface diffusion. Furthermore, solvent−crystal interactions affect the formation of etched pits and play a role in determining the detachment and surface diffusion of surface molecules. As the solid−liquid interaction increases, the ratio of detachment during diffusion increases, and the difference in the contributions of the attachment energies on etching pattern formation is attenuated.

* To whom correspondence should be addressed. Telephone: (765) 496-3387. E-mail: morris@pharmacy.purdue.edu.

11220 *J. Phys. Chem. B, Vol. 108, No. 30, 2004*

Wen et al.

The experiments logically assume that solvent molecules are adsorbed on the crystal surface during the dissolution process.[11] If a solvent molecule can recognize a surface site and participate in the supramolecular motif of the crystal surface, it may alter the original interaction network and, in turn, change the etching pattern. The dissolution mechanism at the crystal surface must include contributions from the solvent−solid interaction, the crystal structure, and the mutual recognition between solvent molecules and molecules in the dissolving lattice.

The attachment energy concept for crystal morphology was proposed by Hartman and Perdok as *periodic bond chain (PBC) theory*.[12−14] In the current research, attachment energies were calculated using Cerius[2] software based on the crystal structures acquired from the Cambridge Structural Database[2,10] and appropriately selected force fields. A key extension of the earlier hypothesis is the assumption that even if two molecules are not on the same face of interest the contribution of the attachment energy between a subsurface molecule and a surface molecule may play a role. By projecting those PBC vectors of the attachment energies on the faces of interest, all the attachment energies related to the face of interest may be calculated. Our original analysis showed that there is more elongation in the direction of stronger attachment energy than in the direction with weaker attachment energy in the etching patterns.[15] This is despite the unaccounted for factors of the temperature effects on attachment energies and surface diffusion. Thus, comparing the etching patterns with the directionality and strength of attachment energies can help to determine what cutoff distance in the attachment energy calculations is necessary to describe the impact on surface diffusion of the crystal's supramolecular interaction network.

In the research reported here, AFM was used to scan the crystal surface and acquire three-dimensional surface images in high resolution. AFM has been successfully used to observe the crystal growth of macromolecules.[16,17] Reyhani et al. have also successfully monitored calcite growth and inhibition using AFM at contact mode in an in situ fluid cell.[18] AFM has been shown to be a very useful tool in providing high-resolution three-dimensional images of crystal surfaces.[19−24]

Studying etching pattern changes in different solvents facilitates testing of the hypotheses and may increase understanding of the interactions between drug and solvent in the dissolution process. The interactions should be the same as those existing in the crystallization process (although the relative contributions will certainly vary). Understanding of dissolution on the molecular level may help to understand the variation of the dissolution rate with crystal faces and lead to the design and control of desired morphologies. In addition, it may aid in choosing suitable solvents or additives that can influence or control habits and/or forms.

Experimental Section

PBC Calculation. The PBC vectors of aspirin and α-glycine crystals were calculated with Cerius[2] 4.2 (Molecular Simulations, Inc., San Diego, CA) based on the crystal structures from the Cambridge Structural Database. The parameters for aspirin[10] (ACSALA01) are the following: $P2_1/c$; $a = 11.43$ Å; $b = 6.59$ Å; $c = 11.40$ Å; $\beta = 95.68°$. The parameters for α-glycine[2] (GLYCIN02) are the following: $P2_1/n$; $a = 5.10$ Å; $b = 11.97$ Å; $c = 5.46$ Å; $\beta = 111.70°$. After the current energy was determined, PBC vectors were calculated using Dreiding 2.21 as the force field; the partial atomic charges were calculated with the equlibrium method, by use of Gasteiger-Quanta 1.0; and the van der Waals interaction and Coulomb force were calculated by use of Ewald summation.

TABLE 1: Etching Agents and Etching Duration for Aspirin (100) Face and α-Glycine (010) Face

	etching duration (s)	
etching agent	aspirin (100)	α-glycine (010)
H_2O	30	15
CH_3COCH_3	5−10	1−3[a]
$(CH_3CO)_2O$	30	N/A[b]
$CH_3COOC_2H_5$	5−10	N/A
$ClCH_2CH_2Cl$	20	N/A
C_5NH_5/CCl_4 (1:5 v/v)	4−5	N/A

[a] 1−3 h. [b] N/A, no visible etching pattern after etching for more than at least 1 h.

Single-Crystal Preparation. A sample of 62.5 g of glycine (Mallinckrodt Baker Inc., Paris, KY) was dissolved in 200 mL of water by heating under stirring in a 400 mL beaker. The supersaturation ratio of glycine at 25 °C was 0.25. The beaker was left at room temperature and covered with film. The water evaporated slowly through the holes punched in the film. After 1 week, α-form single crystals were collected, and the average size was about 1−2 mm.

A sample of 9.0 g of aspirin (Aldrich Chemical, Milwaukee, WI) was dissolved with 50 mL of acetone (EM Science, Gibbstown, NJ) in a beaker at room temperature, and left to evaporate solvent slowly. After 2 days, crystals were collected, and crystal size was about 2−3 mm in diameter.

Single-Crystal X-ray Measurement. The indices of single crystals were determined by a powder X-ray diffractometer (XRD-6000, Shimadzu, Kyoto, Japan). The measured single crystal was mounted onto one AFM sample disk, and the AFM disk was placed on the X-ray diffraction sample holder. Generally, the scan range was from 10° to 40° with a step size of 0.02°. The voltage and current were set at 40.0 kV and 40.0 mA, respectively. The X-ray diffraction patterns were compared with the X-ray powder diffraction patterns simulated by Cerius[2] 4.2 by setting the wavelength to 1.5418 Å, i.e., the radiation wavelength of the diffractometer.

Axis Identification. After the faces of interest were indexed, the directions of the related axes still needed to be determined. The aspirin crystals grown from acetone were plate shaped. Even though a crystal of aspirin exhibited more than two faces, the two faces (100) and (001) along the long dimension were used for axis identification. Therefore, as to the (100) face of aspirin, the *b*-axis was along the long dimension, and the *c*-axis was perpendicular to the long dimension direction.

For α-glycine crystal, if the face next to the (010) face along the longer dimension was the (110) face, then the *c*-axis was along the longer dimension direction; if the face next to the (010) face along the long dimension was the (011) face, then the *a*-axis was along the longer dimension. For most crystals, the *c*-axis was the long dimension. After determination of the *a*- or *c*-axis, the other axis could be determined by comparing the surface morphology with the simulated (010) surface morphology.

Etching. Six solvents used for etching included deionized distilled water, acetone (EM Science, Gibbstown, NJ), ethyl acetate (Mallinckrodt Baker, Paris, KY), acetic anhydride (Aldrich Chemical, Milwaukee, WI), 1,2-dichloroethane (Aldrich Chemical, Milwaukee, WI), pyridine (Aldrich Chemical, Milwaukee, WI), and carbon tetrachloride (Aldrich Chemical, Milwaukee, WI). The dissolution tests were done at room temperature, and the experimental conditions for partial dissolution are listed in Table 1. The single crystals for dissolution tests were attached on AFM disks. After a predetermined time, a disk was taken from the solution, and the remaining solution
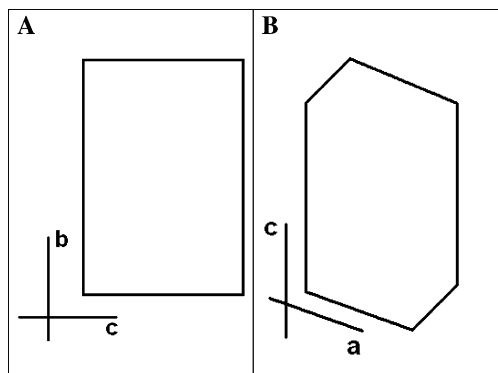
Dissolution of Aspirin and α-Glycine Crystals

J. Phys. Chem. B, Vol. 108, No. 30, 2004 **11221**

Figure 1. Surface morphology and directions of the axes for (A) aspirin (100) face and (B) α-glycine (010) face.

on the crystal surface was removed with a filter paper. Compressed air was used to further remove residual solution from the crystal surface. Finally, the sample was air-dried a while before AFM observation.

AFM Measurement. The surfaces of aspirin and α-glycine single crystals were observed with an AFM (NanoScope Multi-Mode AFM, Digital Instruments, Inc., Santa Barbara, CA). AFM observations were carried out in contact mode at room temperature using a J-type piezo-scanner, and the tips were standard silicon nitride probes. For each observation, images in both the deflection mode and the height mode were saved. The images in the following sections were in the deflection mode unless otherwise specified.

Results and Discussion

The basic approach employed is to determine the PBCs for the crystal structures, projecting them onto the faces of interest and determining the impact on surface diffusion. As discussed in our previous paper,[15] the etching patterns are partially predicted based on the PBCs in different directions within the face, as the detachment is energy related. The probability of detachment can be exponentially related to the corresponding energy. By comparing the predicted etching patterns with the observed etching patterns, the interactions between solvent molecules and drug molecules at the crystalline interface can be better understood. Both the solubilizing ability and potential surface adsorption of solvents may affect the formation of etching patterns, and the changes can help elucidate the dissolution process.

Preparation of Single Crystals of Aspirin and α-Glycine. Aspirin single crystals were grown under isothermal conditions from a supersaturated acetone solution. Even though the (100) face was exhibited as a growth face, to get a molecularly smooth surface, the (100) face was generated by cleaving the crystals with a needle and checking them under a microscope to pick those crystals with smooth surfaces. The surface morphology and the directions of the axes for aspirin (100) face are shown in Figure 1A. Figure 2A shows the powder X-ray diffraction pattern for the (100) face of aspirin single crystal.

α-Glycine single crystals were grown from supersaturated water solution and exhibited three major faces: (110), (011), and (010). Similar to the (100) face of aspirin, a molecularly smooth (010) face was also generated by cleaving α-glycine single crystals with a needle and checking them under a microscope. The surface morphology and the directions of the axes for α-glycine (010) face are shown in Figure 1B. Figure 2B shows the X-ray diffraction for the (010) face of α-glycine single crystals. Before etching, both the (100) face of aspirin

and the (010) face of α-glycine crystals were examined by AFM to confirm the smoothness at the 3 nm level and the absence of preexisting patterns.

Crystal Structures and Attachment Energies on Related Faces. The molecular structures of aspirin and glycine are shown in Figure 3. For aspirin, there is no hydrogen bond chain, and there are two-dimensional layers stacked along the *a*-axis and along the *c*-axis, which explains why the crystals can easily be cleaved to yield (100) and (001) faces, respectively.[10] In α-glycine crystal, each molecule has several hydrogen bonds with neighboring molecules, and all the hydrogen bonds are of the N−H−O−C type[2]. The two-dimensional layers formed by the hydrogen bonding network are stacked along the *b*-axis, and there are only Van der Waals interactions between layers. Therefore, the (010) face is an easily cleavable face as all the hydrogen bond chains exist within the (010) face.

The PBC vectors for both crystals were calculated with Cerius[2]. The unit cell of each has four molecules (i.e., $Z = 4$), and their geometric centers of mass were used to determine the directions of the PBC vectors. For both crystals, because the lengths of the *a*-, *b*-, and *c*-axes are not equal, a transformed coordinate system was used to facilitate the calculation of the PBC vector projections on different faces. In the new simplified system, the unit vectors **A**, **B**, and **C** are in the original direction of the *a*-, *b*-, and *c*-axes, respectively, but with unit length for each crystal (basically fractional coordinates). The calculation procedure is detailed in our previous research paper.[15]

Figure 4 shows the PBC vectors of aspirin crystal. Among the vectors, the second strongest PBC is parallel to the (100) face, because the second strongest PBC is along the *b*-axis and the *b*-axis is parallel to the (100) face. The PBC vectors have been projected onto the (100) face, and the 12 largest projections that comprise more than 95% of the total projections were chosen for further analysis. In Table 2, the projections of the PBC vectors are listed clockwise to show the energy distribution in different directions on the (100) face. The largest repulsive projection is 0.31 kcal/mol, which is much smaller than the smallest attractive projection of −1.15 kcal/mol. Thus the effects of the repulsive projections are ignored in the current treatment. Because the *b*-axis is perpendicular to the *c*-axis in the aspirin cell, the new unit vectors **B** and **C** have been used as the orthonormal bases for the (100) face in the calculation. The perpendicular components of the first and third strongest PBC vectors are much larger than their projections on the (100) face, and the second strongest PBC vector is parallel to the (100) face. Overall, on the (100) face of aspirin, by checking the projections in different directions, the dominant attachment energy direction is along the *b*-axis, with weaker energies along the *c*-axis as well as in the intermediate between the *b*- and *c*-axes.

Figure 5 shows the main PBC vectors of α-glycine crystals, and among the vectors, the second strongest PBC is parallel to the (010) face. The PBC vector projections on the (010) face were calculated, and the 17 largest projections that are larger than 10% of the maximal projection of 10.4 kcal/mol were chosen for further analysis. In Table 3, the projections of the PBC vectors are also listed clockwise to show the energy distribution in different directions on the (010) face. Unlike the case for aspirin crystals, the repulsive projections cannot be ignored in α-glycine crystals. For the first, third, and fourth strongest PBC vectors, their projected components are approximately the same as the perpendicular components; i.e., these vectors cross the (010) face obliquely. The second and
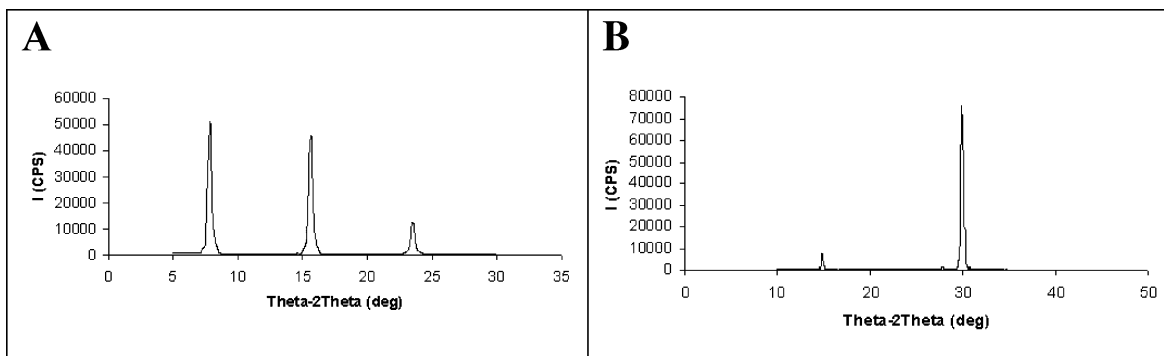
Figure 2. X-ray diffraction of (A) aspirin (100) face and (B) α-glycine (010) face. (A) The 2θ values for the three peaks are 7.8079°, 15.6030°, and 23.4841° with corresponding faces (100), (200), and (300). (B) The 2θ values for the two peaks are 14.8204° and 29.8882° with corresponding faces (020) and (040).
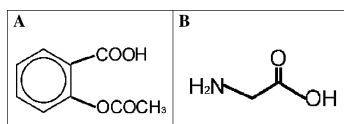

Figure 3. Molecular structures of aspirin (A) and glycine (B).

fifth strongest PBC vectors are parallel to the (010) face: the second strongest PBC follows exactly the *c*-axis and the fifth strongest PBC is approximately between the *a*-axis and the *c*-axis. The fourth PBC vector's projection is mainly in the *a*-axis direction. Overall, on the (010) face, the dominant attachment energy is along the *c*-axis, with weaker attachment energy along the *a*-axis.

Etching Patterns on the (100) Face of Aspirin Crystals. The six solvents used in the etching experiments were water, acetone, ethyl acetate, acetic anhydride, pyridine, and dichloroethane. Etching patterns of aspirin crystals created by different solvents are shown in Figures 6 and 7. The patterns are elongated along the *b*-axis and/or the *c*-axis depending upon the solvent.

To compare the observed etching patterns on the (100) face with the patterns predicted from the projected PBC vectors, a graphical method illustrated in Figure 8 was employed. The relative strength of attachment energies in different directions is plotted against the direction. On the (100) face, the projected energies are mainly distributed in three directions: **B**, between **B** and **C** (equivalent to between −**B** and −**C**), and between **B** and −**C**, where the three dominant directions can form a triangle. This is significant as there are triangular patterns exhibited in the etching patterns produced with water, acetone, ethyl acetate, and acetic anhydride; i.e., the etching patterns follow attachment energy directionality. Li et al.[11] demonstrated that surface diffusion of crystal molecules is very important for the formation of the etching patterns. Our previous paper[15] showed that the distribution of projection energy in different directions influences the surface diffusion process and affects the etching pattern formation. Therefore, the consistency between the etching pattern and the distribution pattern of energy projections on the (100) face further supports the idea that surface diffusion is significantly influenced by the projections of attachment energies on the face.

To compare the relationship between the exhibited etching patterns and the main projected energies, the three directions with relative major attachment energies on the (100) face have been taken into consideration, and the main features of predicted etching patterns have been compared with the observed etching patterns. Because the probability of the detachment process can be related to the attachment energy, the length (*L*) of etching

pits in the corresponding direction has been expressed as[15]

$$L_i = A \, \exp\!\left(\frac{E_i}{B}\right) \quad (1)$$

E_i is the attachment energy in the corresponding direction; A and B are constants related to temperature, solvents, etc. At constant temperature, a solvent with higher solubilizing ability will have a larger B value.[15] The length ratios of etching pits in different directions can be expressed as

$$\frac{L_i}{L_j} = \exp\!\left(\frac{E_i - E_j}{B}\right) \quad (2)$$

The projection of attachment energy can be considered as energy with direction, i.e., a vector. By summing the vectors around the specified directions, the combined energies have been approximately calculated. Table 2 shows that the approximate combined energy is 14 kcal/mol in the **B** direction, 7 kcal/mol in the direction between **B** and **C**, and 7 kcal/mol in the direction between **B** and −**C**. Based on eq 2, Figure 9 shows the main features of the predicted etching patterns under different B values. As the value of B increases, the length differences of etching pits in different directions become smaller.

Along the *b*-axis, all the features are relatively straight except for the water-induced etching pattern; along the *c*-axis, the patterns are highly solvent dependent. Two solvent-related aspects, the solubilizing ability of solvent and adsorption of solvent onto crystal surface, may affect the formation of etching patterns. For stronger solvents, the simulation model[11] shows that stronger solid−liquid interaction will cause the etching pattern in the direction of dominant attachment energy to be attenuated relative to that for weaker solid−liquid interaction. For weaker solvents, the detached molecules should have more time to diffuse on the crystal surface and make the detachment and attachment occur more for each finally dissolved molecule; thus, strong attachment energies play a relatively more important role in controlling surface diffusion.

The rank order of measured solubilities of aspirin at 25 °C in different solvents, as shown in Table 4, is in the order pyridine > acetone > acetic anhydride > ethyl acetate > dichloroethane > water. Except water, the effects of solvents on the elongation along the *c*-axis follow the order of their solubilizing ability for aspirin. For dichloroethane, the etching patterns are very similar to the etching patterns predicted in Figure 9 with $B =$ 5. Because dichloroethane cannot form hydrogen bonding interactions with aspirin on the crystal surface, the longer surface diffusion time of aspirin determined by the weak solubilizing ability makes the detachment and attachment occur more
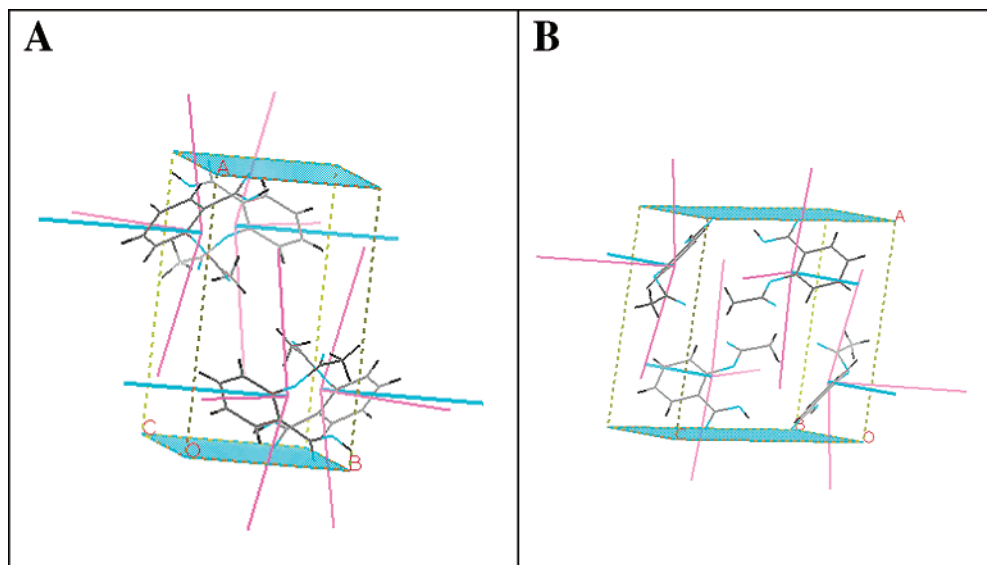
Dissolution of Aspirin and α-Glycine Crystals

J. Phys. Chem. B, Vol. 108, No. 30, 2004 **11223**

Figure 4. Periodic bond chains of aspirin crystals calculated with Cerius². The light blue faces in both (A) and (B) are (100) faces. The blue lines represent the second strongest PBC, and purple lines represent other PBCs.

TABLE 2: Projections of 12 Dominant PBC Vectors on the Aspirin (100) Face and in the Direction Perpendicular to the Aspirin (100) Face Sorted by Angles[a]

		energy (kcal/mol)			
PBC	Proj	B	C	Perp	angle (deg)
−1.51	−1.1752	−0.1072	0.9942	−0.9482	−83.8858
−3.94	−3.6039	0.3974	−0.9177	−1.5923	−66.6192
−3.55	−2.3838	−0.5660	0.8244	−2.6306	−55.5552
−2.98	−2.8961	0.8640	−0.5034	−0.7020	−30.2437
−2.32	−1.5750	0.9981	−0.0609	−1.7034	−3.4924
−5.36	−3.8153	0.9981	−0.0609	−3.7647	−3.4924
−7.47	−7.4700	−1.0000	0.0000	0.0000	0.0000
−1.79	−1.4586	−0.9990	−0.0439	−1.0376	2.5169
−6.28	−1.1595	−0.9540	−0.2997	−6.1720	17.4465
−11.4	−2.2992	−0.9540	−0.2997	−11.165 7	17.4465
−5.83	−5.4733	−0.6477	−0.7619	−2.0078	49.6562
−2.88	−2.1790	−0.5158	−0.8567	−1.8832	58.9768

ᵃ The **B** vector and **C** vector are orthonormal bases of the (100) face, and are used here to show the directions of the projected PBC vectors. PBC, attachment energy of the PBC vector; Proj, projected energy on the (100) face; Perp, projected energy along the direction perpendicular to the (100) face; angle, angle between the projection vector and **B** vector.

frequently for each dissolved aspirin molecule; thus the etching patterns are mainly controlled by the major attachment energies along the *b*-axis.

For the etching patterns produced by those solvents with moderate solubilizing ability (acetic anhydride and ethyl acetate) as well as by water, there exist visible triangular patterns to varying degrees similar to the predicted etching patterns in Figure 9 when *B* = 20. The moderate solvents cause the surface diffusion time to decrease and *B* values to increase; thus weaker attachment energies play a more important role in etching pattern formation than in weak solvents. For water, the hydrogen bonding interactions between water and aspirin crystal surface may cause aspirin molecules diffusing on the surface to be difficult to incorporate into crystal again, and to make the detachment and attachment occur less frequently for each dissolved aspirin molecule. The decreased detachment and attachment frequency in water results in etching patterns similar to the etching patterns by those moderate solvents.

For strong solvents such as acetone and pyridine, surface diffusion time is relatively shortened. In the strong solvents,

directions of weaker attachment energies also need to be taken into consideration. For example, the attachment energies in the **C** direction (Figure 8) may contribute to the etching patterns along the *c*-axis by acetone and pyridine. Overall, the effects of solvent solubilizing ability on the impact of the attachment energy on surface diffusion and etching pattern formation are manifested in the *B* value of eq 2.

The observed depths of the etching patterns are not symmetric along the *c*-axis. Figure 10 shows the height profiles for the etching patterns by pyridine and dichloroethane. Among the seven dominant PBC vectors shown in Table 2, all but the second strongest PBC are across the (100) face more or less, which may cause the etching depth to change along the *c*-axis.

All the solvents except dichloroethane are able to form hydrogen bonds with host aspirin molecules. However, because there is no hydrogen bond chain in aspirin crystals, adsorption through hydrogen bonds may not disrupt the dissolution directionality as effectively as in acetaminophen.[11] The aspirin dimers formed though carboxylic acid hydrogen bonds are aligned partially in the *b*-axis direction, but the etching patterns along the *b*-axis are straight with the exception of slight variations with water. Even though the effects of solvent adsorption on surface diffusion cannot be excluded, the etching patterns produced by the six solvents suggest that the solvent adsorption is less important in this system (i.e., the attachment energy effects dominate).

Etching Patterns on the (010) Face of α-Glycine Crystals. Only water and acetone were used in the α-glycine etching experiments due to the limited solubility of glycine in the other solvents, showing no visible etching patterns after 12 h. The etching patterns produced by water and acetone are shown in Figure 11, and the corresponding height profiles are shown in Figure 12. The images show that the etching patterns elongated more along the *c*-axis than along the *a*-axis.

Table 3 shows that the second strongest PBC is along the *c*-axis, and the first and third strongest PBCs have approximately same projected energies as perpendicular energies. On the (010) face, the projected attachment energy is significant in three directions: the combined energy is approximately 11 kcal/mol in the direction of the *c*-axis, 7 kcal/mol in the direction of the *a*-axis, and 10 kcal/mol in the direction of 40°. The projection in the direction of 64° is partially reduced by the repulsive
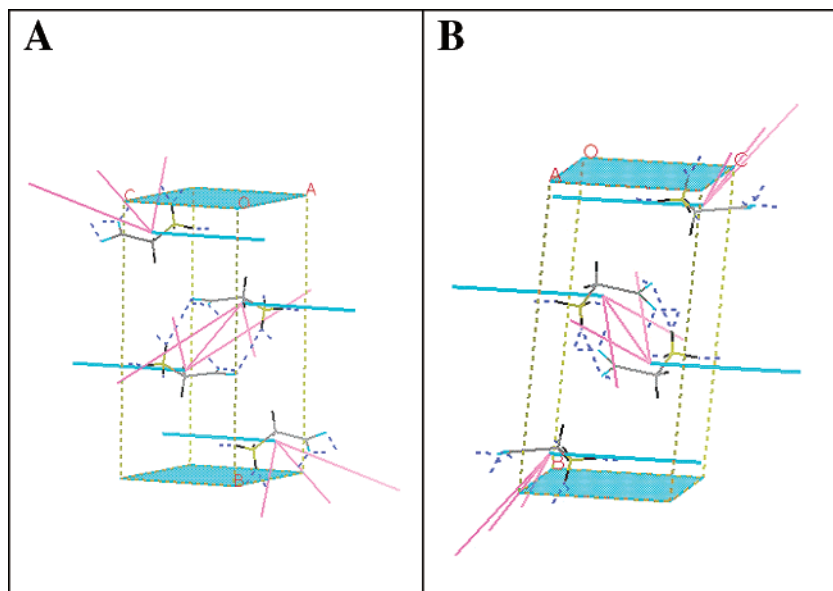
Figure 5. Periodic bond chains of α-glycine calculated with Cerius². The light blue faces in both (A) and (B) are the (010) faces. The blue lines represent the second strongest PBC vector, and purple lines represent other PBC vectors.

TABLE 3: Projections of 17 Dominant PBC Vectors on the α-Glycine (010) Face and in the Direction Perpendicular to the α-Glycine (010) Face (i.e., the *b*-Axis Direction) Sorted by Angles[a]

PBC	energy (kcal/mol)				angle (deg)
	Proj	A	C	Perp	
−3.9500	−3.6985	−0.8447	0.1982	−1.3870	−75.8635
−1.5700	−1.4808	−0.7996	0.2853	−0.5216	−69.0256
−2.2200	−2.2200	−1.0000	0.0000	0.0000	−68.3000
−11.7700	−8.1262	−0.4257	0.4084	−8.5146	−44.1060
−2.4800	−2.4800	−0.5834	0.6246	0.0000	−40.9767
−2.2400	−1.8117	−0.4718	0.5051	−1.3173	−40.9767
−1.1900	−1.1277	−0.2561	0.8226	−0.3799	−16.1440
1.9400	1.4734	0.0976	−0.7179	1.2620	−7.2066
−10.4100	−10.4100	0.0000	−1.0000	0.0000	0.0000
−1.7200	−1.5876	−0.3087	−0.9915	−0.6618	16.1440
1.5200	1.1996	−0.3614	−0.8480	0.9334	21.6142
2.9100	2.6778	0.4809	0.9824	1.1390	24.4713
−1.5100	−1.1016	−0.4802	−0.7549	−1.0328	30.6006
1.4400	1.3561	−0.8094	−0.8665	0.4842	40.9767
−2.0200	−1.4246	0.7106	0.5111	−1.4321	52.2836
−6.8500	−5.1627	0.8075	0.3711	−4.5021	63.7195
3.7200	3.3959	−0.9825	−0.3506	1.5185	69.0256

[a] The vectors **A** and **C** are in the *a*- and *c*-axis directions but with unit length. The vectors **A** and **C** are not the orthonormal bases of (010) face because β is not equal to 90°. PBC, attachment energy of the PBC vector; Proj, projected energy on the (010) face; Perp, projected energy along the direction perpendicular to the (010) face; angle, angle between projection vector and **C** vector.

projection in the direction of 69°, and is thus ignored. The etching pattern in the direction of the *c*-axis is longer than that in the direction of the *a*-axis, which is consistent with the phenomenon that the attachment energy along the *c*-axis is stronger than along the *a*-axis.

To compare the relationship between the observed etching patterns and attachment energy projections on the (010) face of α-glycine, eq 2 was again used to predict the etching pattern. Note the angle between the *a*-axis and the *c*-axis is 111.7° (i.e., −68.3°). Figure 13 shows the main features of the predicted dominant etching patterns with and without considering the effects of 40° projections. When the effects of 40° projections are not considered, the predicted etching patterns fit the observed etching patterns very well.
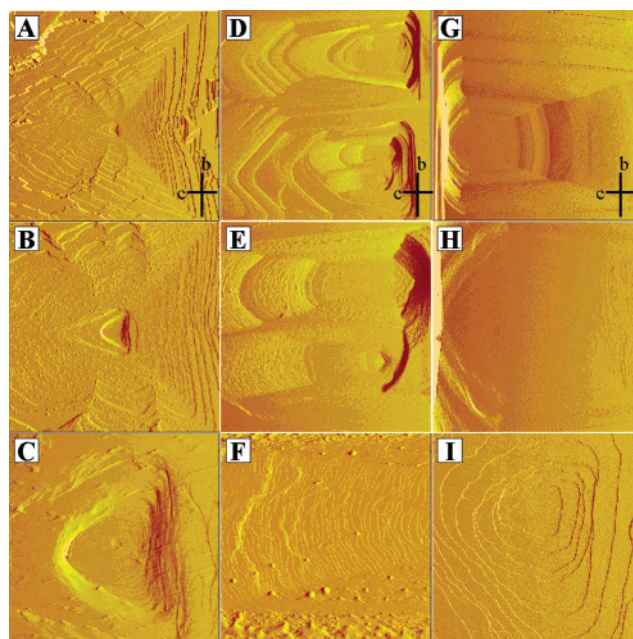

Figure 6. AFM images of the aspirin (100) face etched by water (A−C), acetone (D−F), and ethyl acetate (G−I). The image sizes are (A, D, G) 60 × 60 μm², (B, E, H) 20 × 20 μm², and (C, F, I) 5 × 5 μm², respectively. From (A) to (C), (D) to (F), and (G) to (I) the images were zoomed in gradually. Directions of the *b*-axis and *c*-axis are shown on (A), (D), and (G).

There is a problem in fitting the predicted etching patterns with observed etching patterns: the effects of the projections of 40° have not been observed. Solvent adsorption may be a factor, because glycine crystals grown from water have a morphology significantly different from that of glycine crystals grown from sublimation. Lahav et al.[25] suggested that glycine−solvent interaction should be taken into consideration based on the hydrophilicity of glycine crystal in different directions. The strongest PBC that contributes to the projection of 40° is mainly determined by hydrogen bonding interactions; however, the molecules forming the hydrogen bonds do not belong to one hydrogen bond chain (there is no hydrogen bond chain across the (010) face). The detachment of one glycine molecule in the
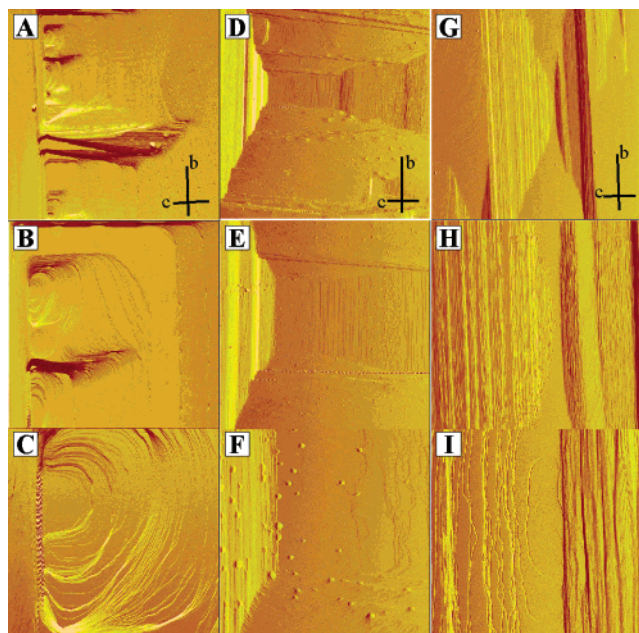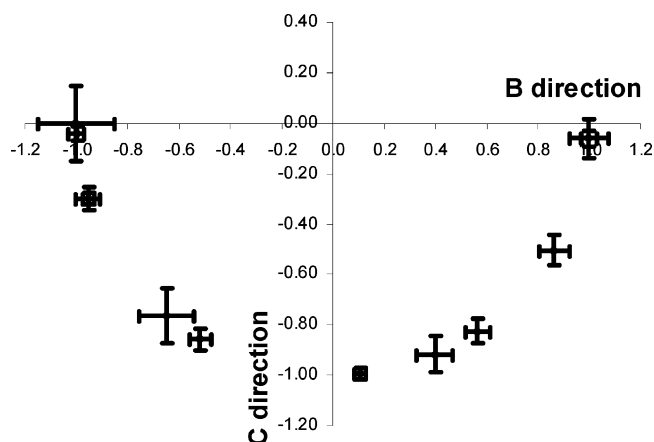
Dissolution of Aspirin and α-Glycine Crystals

J. Phys. Chem. B, Vol. 108, No. 30, 2004 **11225**

Figure 7. AFM images of the aspirin (100) face etched by acetic anhydride (A−C), pyridine (D−F), and dichloroethane (G−I). The image sizes are (A, D, G) 60 × 60 μm², (B, E, H) 20 × 20 μm², and (C, F, I) 5 × 5 μm². From (A) to (C), (D) to (F), and (G) to (I) the images were zoomed in gradually. Directions of the *b*-axis and *c*-axis are shown on (A), (D), and (G).

Figure 8. Relationship of projected energies on the aspirin (100) face with **B** and **C** directions. The standard error bars have been used to represent the relative energy strength.
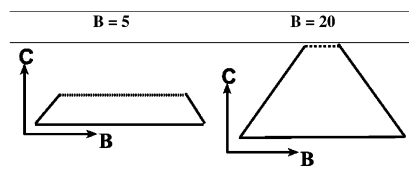

Figure 9. Predicted etching patterns of aspirin (100) face under different *B* values.

Figure 10. Height profiles of aspirin etching patterns by pyridine and dichloroethane. The top height profile, taken along lines on the middle-left height image, corresponds to the deflection image in Figure 7E and is for the etching pattern by pyridine. The bottom height profile, taken along lines on the middle-right height image, corresponds to Figure 7H and is for the etching pattern by dichloroethane.

TABLE 4: Solubility of Aspirin in Different Solvents

solvent	solubility (mg/mL)
water	3.83
dichloroethane	10.6
ethyl acetate	65.8
acetic anhydride	143
acetone	167
pyridine	>376

direction of 40° may not only disrupt the hydrogen bond chain, but may also disrupt the packing, which may cause the effects of 40° to be unobserved. So far the exact reason for the discrepancy is unknown, and more study is underway to further elucidate the process. However, the strongest projections in the **C** direction do have clear effects on the etching pattern in the direction of the *c*-axis, and the third strongest projections in the *a*-axis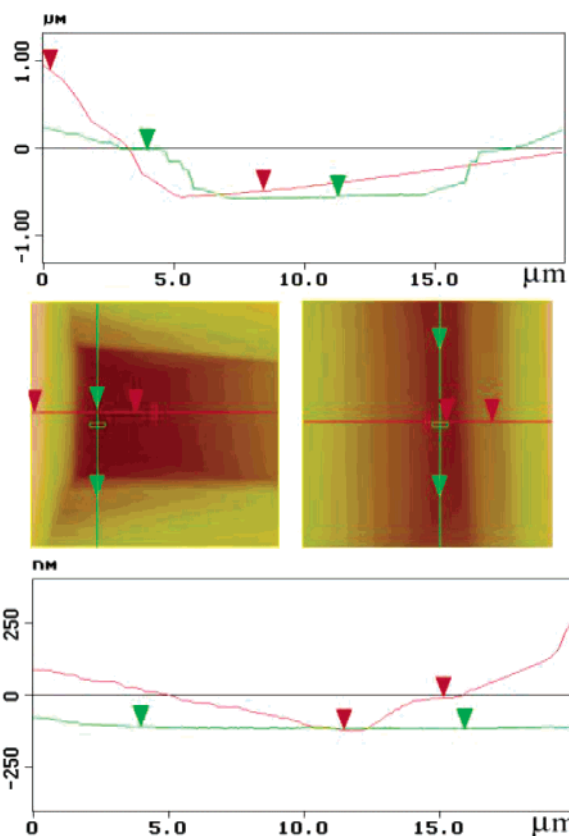 direction also impact on the etching patterns. This is consistent with the hypothesis that surface diffusion is being guided by the attachment energy network.

The multiple hydrogen bond chains in the three-dimensional structure of α-glycine crystal suggest that glycine may form hydrogen bonds with acetone in many directions. In the crystal, the hydrogen bond network in each layer along the *b*-axis is composed of hydrogen bond chains, and the adsorption of acetone onto the crystal surface may disrupt some hydrogen bond chains by forming a hydrogen bond with a glycine molecule in the lattice but failing to continue the chain (as it cannot donate a proton). The surface adsorption of a poor solvent on a crystal surface may cause surface diffusion to decrease in the strong adsorption direction(s). In the partial dissolution experiments, only 15 s was needed for water to create clear etching patterns in contrast to the 1−3 h needed for acetone. Because water has much higher solubilizing ability than acetone for glycine, the ratio of the length in the *c*-axis versus the length in the *a*-axis should be significantly larger in acetone (weak solvent) according to eq 2. However, the difference of the ratios in water and acetone is not significant, which may indicate a larger impact of solvent adsorption. As the potential adsorption of acetone has many possible directions, surface diffusion and
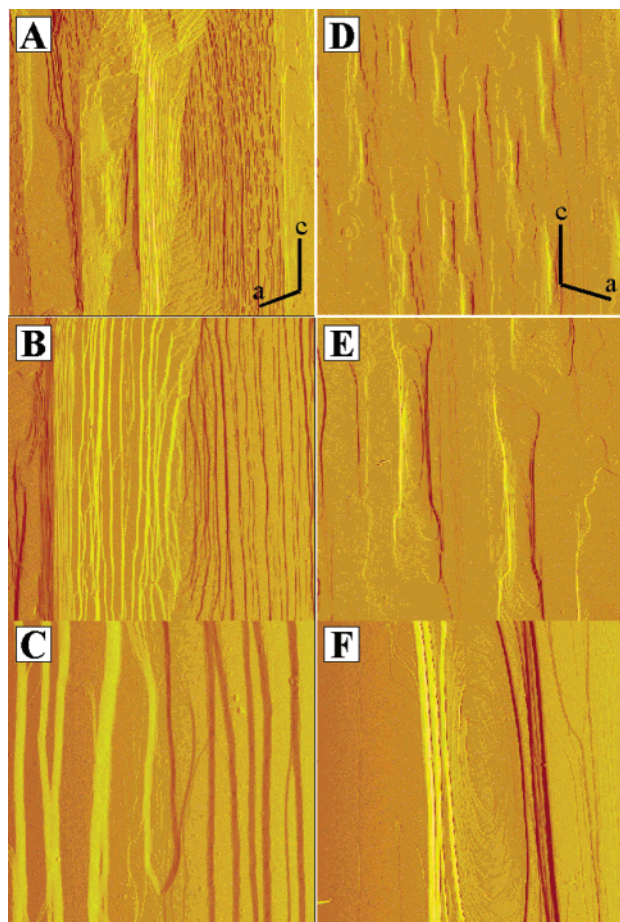
11226 *J. Phys. Chem. B, Vol. 108, No. 30, 2004*

Wen et al.

Figure 11. AFM images of the α-glycine (010) face etched by water (A−C) and acetone (D−F). The image sizes were (A, D) 60×60 μm^2, (B, E) 20×20 μm^2, and (C, F) 5×5 μm^2. From (A) to (C) and (D) to (F) the images were zoomed in gradually. Directions of the a-axis and c-axis are shown on (A) and (D).

Figure 12. Height profiles of α-glycine etching patterns by water and acetone. The top height profile, taken along lines on the middle-left height image, corresponds to the deflection image in Figure 11B and is for the etching pattern by water. The bottom height profile, taken along lines on the middle-right height image, corresponds to Figure 11E and is for the etching pattern by acetone.

Figure 13. Predicted etching patterns of α-glycine (010) face (A) without and (B) with considering the effects of 40° projections. Assume B value to be 3.

the resulting etching pattern may be affected in many directions. By combining surface diffusion guided by the PBCs with the contribution of solvent adsorption, the oval shape etching patterns by acetone may still be addressed based on the projected PBC vectors if the specific interactions of the solvent with the surface are understood.

Figure 12 also shows that the etching patterns produced by acetone are much deeper than the etching pattern produced by water. Similar behavior has been observed for acetaminophen etched with dichloroethane relative to the patterns observed with five other solvents. Solvent surface adsorption may also affect the detachment of the α-glycine molecules in contact with adsorbed solvent by a mechanism still under investigation.

Conclusions

The etching patterns produced on the aspirin (100) and α-glycine (010) faces with different solvents follow the direction and are proportional to the strength of the major attachment energies projected onto the faces of interest. This supports the contention that, for both aspirin and α-glycine, etching patterns are mainly controlled by the crystal structures; i.e., surface diffusion during the dissolution process is guided by the intrinsic interaction network.

The solubilizing ability of solvents also plays a very important role in determining the relative significance of attachment energies in different directions. The comparison of the etching patterns on the aspirin (100) face, produced by different solvents,
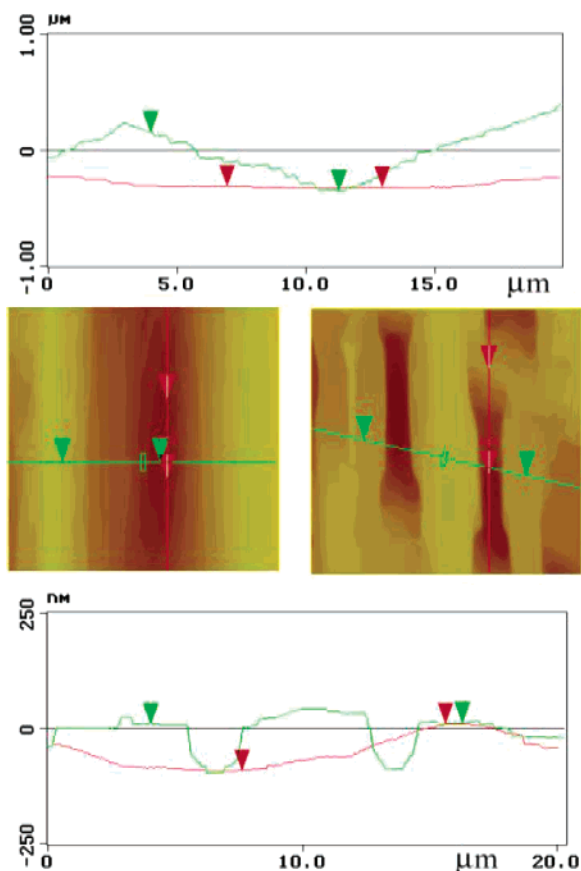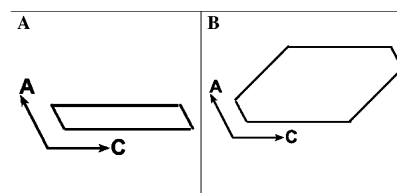
shows that as the solubilizing ability of solvents increases the effect of strong attachment energy on surface diffusion is relatively decreased (there is less discrimination in attachment energy as the solvent−solute energy increases). The predicted etching patterns match well with observed etching patterns especially for the solvents with weak and moderate solubilizing ability. For solvents with high solubilizing ability (e.g., acetone, pyridine), more minor attachment energies must be taken into account to obtain predicted etching patterns that can match observed etching patterns.

Even though solvent surface adsorption may not play a dominant role in the formation of etching patterns for the aspirin (100) face and α-glycine (010) face with "good" solvents, the effects cannot be ignored for "poor" solvents. Acetone molecules may adsorb onto the α-glycine (010) face through hydrogen bonding with glycine molecules in the same layer. The adsorption may cause the etching pattern to adopt an oval shape due to the inhibition on surface diffusion in many directions. This

adsorption process may also cause the α-glycine (010) etching pattern to be relatively deeper than the etching pattern by water.

The model assumes that the growth and dissolution unit is a single molecule. It also only implicitly builds in the concepts of solvation through the solubilization ability of the solvent. The attachment energy is assumed here to be the primary factor controlling the process, and the deviations seen in the logarithmic model in fact are due to these factors. For the α-glycine (010) face, the effects of the 40° projections have not been observed, and the reason is not clear. Some effects may play unanticipated roles, such as solvent adsorption, hydrogen bond chain, and disruption of crystal lattice.

References and Notes

(1) Payne, R. S.; Rowe, R. C.; Roberts, R. J.; Charlton, M. H.; Docherty, R. *J. Comput. Chem.* **1999**, *20*, 262.

(2) Marsh, R. E. *Acta Crystallogr.* **1958**, *11*, 654.

(3) Iitaka, Y. *Acta Crystallogr.* **1961**, *14*, 1.

(4) Iitaka, Y. *Acta Crystallogr.* **1960**, *13*, 35.

(5) Peeters, A.; Van Alsenoy, C.; Lenstra, A. T. H.; Geise, H. J. *J. Chem. Phys.* **1995**, *103*, 6608.

(6) Watanabe, A.; Yamaoka, Y.; Takada, K. *Chem. Pharm. Bull.* **1982**, *30*, 2958.

(7) Kim, Y.; Matsumoto, M.; Machida, K. *Chem. Pharm. Bull.* **1985**, *33*, 4125.

(8) Danesh, A.; Connell, S. D.; Davies, M. C.; Roberts, C. J.; Tendler, S. J. B.; Williams, P. M.; Wilkins, M. J. *Pharm. Res.* **2001**, *18*, 299.

(9) Danesh, A.; Davies, M. C.; Hinder, S. J.; Roberts, C. J.; Tendler, S. J.; Williams, P. M.; Wilkins, M. J. *Anal. Chem.* **2000**, *72*, 3419.

(10) Kim, Y.; Machida, K.; Taga, T.; Osaki, K. *Chem. Pharm. Bull.* **1985**, *33*, 2641.

(11) Li, T.; Morris, K. R.; Park, K. *J. Phys. Chem. B* **2000**, *104*, 2019.

(12) Hartman, P.; Perdok, W. G. *Acta Crystallogr.* **1955**, *8*, 49.

(13) Hartman, P.; Perdok, W. G. *Acta Crystallogr.* **1955**, *8*, 521.

(14) Hartman, P.; Perdok, W. G. *Acta Crystallogr.* **1955**, *8*, 525.

(15) Wen, H.; Li, L.; Morris, K. R.; Park, K. *J. Phys. Chem. B* **2004**, *108*, 2270.

(16) Land, T. A.; De Yoreo, J. J.; Lee, J. D. *Surf. Sci.* **1997**, *384*, 136.

(17) Wiechmann, M.; Enders, O.; Zeilinger, C.; Kolb, H.-A. *Ultramicroscopy* **2001**, *86*, 159.

(18) Reyhani, M. M.; Oliveira, A.; Parkinson, G. M.; Jones, F.; Rohl, A. L.; Ogden, M. I. *Int. J. Mod. Phys.* **2002**, *16*, 25.

(19) Radenovic, N.; van Enckevort, W. *J. Cryst. Growth* **2002**, *234*, 589.

(20) Shiojima, K. *J. Vac. Sci. Technol., B* **2000**, *18*, 37.

(21) Plomp, M.; van Enckevort, W. J. P.; Vlieg, E. *J. Cryst. Growth* **2000**, *216*, 413.

(22) Mao, G.; Lobo, L.; Scaringe, R.; Ward, M. D. *Chem. Mater.* **1997**, *9*, 773.

(23) Ward, M. D. *Chem. Rev.* **2001**, *101*, 1697.

(24) Carter, P. W.; Hillier, A. C.; Ward, M. D. *Mol. Cryst. Liq. Cryst. Sci. Technol., Sect. A: Mol. Cryst. Liq. Cryst.* **1994**, *242*, 321.

(25) Lahav, M.; Leiserowitz, L. *Chem. Eng. Sci.* **2001**, *56*, 2245.